

The Consequences of Kesterite Equilibria for Efficient Solar Cells

Alex Redinger, Dominik M. Berg,* Phillip J. Dale, and Susanne Siebentritt

University of Luxembourg, Laboratory for Photovoltaics, 41, rue du Brill, L-4422 Belvaux, Luxembourg

S Supporting Information

ABSTRACT: Copper–zinc–tin–chalcogenide kesterites, $\text{Cu}_2\text{ZnSnS}_4$ and $\text{Cu}_2\text{ZnSnSe}_4$ (CZTS(e)) are ideal candidates for the production of thin film solar cells on large scales due to the high natural abundance of all constituents, a tunable direct band gap ranging from 1.0 to 1.5 eV, a large absorption coefficient, and demonstrated power conversion efficiencies close to 10%.¹ However, Sn losses through desorption of SnS(e) from CZTS(e) at elevated temperatures (above 400 °C)^{2–5} impede the thorough control of film composition and film homogeneity. No robust and feasible fabrication process is currently available. Here we show that understanding the formation reaction of the kesterite absorber is the key to control the growth process and to drastically improve the solar cell efficiency. Furthermore, we demonstrate that this knowledge can be used to simplify the four-dimensional parameter space (spanned by the four different elements) to an easy and robust two-dimensional process. Sufficiently high partial pressures of SnS(e) and S(e) (a) prevent the decomposition reaction of the CZTS(e) at elevated temperatures and (b) introduce any missing Sn into a Sn-deficient film. This finding enables us to simplify the precursor to a film containing only Cu and Zn, whereas Sn and S(e) are introduced from the gas phase by a self-regulating process.

The major challenge for cost-effective solar electricity is to provide technologies which enable in a convenient, manufacturable form, the low-cost capture and conversion of sunlight to electrical energy.⁶ Because of their extremely low raw material costs, kesterites can play a major role in such technologies, if it will be possible to define a robust and feasible production process. The most successful procedure to prepare CZTS(e) thin films in terms of solar cell efficiency is a liquid-based process where all constituents are dissolved in a hydrazine solution which is spin coated onto a molybdenum-coated glass substrate followed by a short annealing to 540 °C on a hot plate.¹ A record efficiency of 9.7% has been achieved with this technique, whereas vacuum-based processes show efficiencies lower than 7%.^{7–9} The best performing vacuum-processed devices have been produced by rapid coevaporation⁸ (4.1% CZTS solar cell), by low-temperature coevaporation followed by annealing⁷ (6.8% CZTS), or by annealing precursors in a H_2S atmosphere⁹ (6.7% CZTS). These methods have been developed empirically, and no consensus exists describing the prerequisites to form CZTS(e) thin films suitable for solar cells. We will show here that the key physical mechanism which limits the solar cell performance is the loss

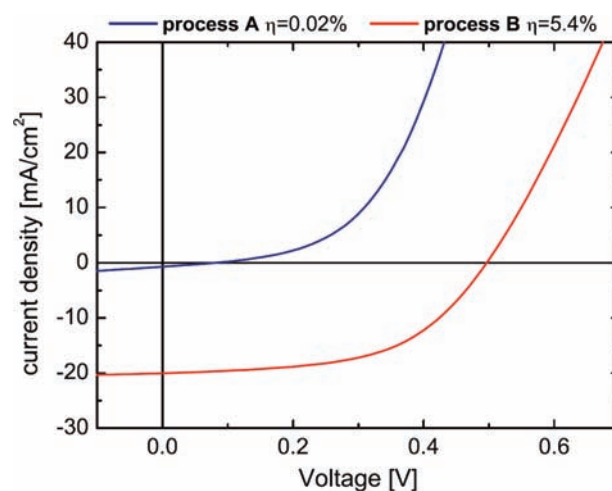


Figure 1. Current–voltage characteristics of two CZT(S,Se) solar cells under illumination. Process A: annealing in sulfur only; process B: annealing in sulfur and SnS(g) .

of Sn. The way to improve the cell performance is to avoid Sn loss by the use of the chemical equilibrium of the decomposition reaction.

Figure 1 shows the solar cell performance of two samples produced by different annealing procedures. Both precursors were formed alike by coevaporation of Cu, Zn, Sn, and Se on Mo-coated glass substrates at a substrate temperature of 330 °C. The composition of both precursors, as deduced from energy dispersive X-ray analysis, was $\text{Cu}/(\text{Sn}+\text{Zn}) = 0.9$, $\text{Zn}/\text{Sn} = 1.1$, close to those observed in the highest efficiency solar cells.^{1,7,9} However, an additional annealing step is mandatory to improve the crystallinity of the thin film. This heat treatment has been performed in a small graphite box in an excess sulfur atmosphere at a temperature of 560 °C for 120 min. This leads to an incomplete substitution of Se by S, a phenomenon well-known from the related $\text{Cu}(\text{In,Ga})(\text{Se,S})_2$ compounds (see, e.g. ref¹⁰). Mixed CZT(S/Se) thin films are currently the best performing devices.¹

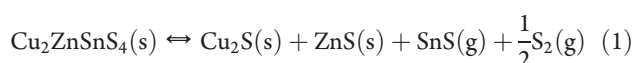
In a first experiment (process A) the film has been annealed in 1 mbar forming gas, and excess elemental sulfur is provided in the form of pellets. The current–voltage characteristics as shown in Figure 1 illustrate that the performance of the device is unacceptable. An efficiency of 0.02%, an extremely small short circuit current $J_{\text{SC}} = 0.72 \text{ mA/cm}^2$ and an open circuit voltage $V_{\text{OC}} = 80 \text{ mV}$ have been observed. In a second experiment (process B¹¹) the annealing procedure has been repeated except

Received: December 29, 2010

Published: February 18, 2011

that an additional 1 mg of Sn was present in the box. Figure 1 shows the drastically improved current–voltage characteristics of the resulting solar cell with an efficiency of 5.4%, a $J_{SC} = 20 \text{ mA/cm}^2$ and a $V_{OC} = 497 \text{ mV}$. The cell exhibits a band gap of approximately 1.2 eV, as indicated by quantum efficiency measurements (see Supporting Information [SI] Figure S2). The performance of the solar cell is limited by a series resistance of $3 \Omega \text{ cm}^2$ similar to other reported CZT(S,Se) devices⁷ (see SI Table 1). The process is reproducible, but no further optimization in terms of composition and annealing procedure has been performed so far. We have prepared solar cells better than the one of process (A) in the past; even by annealing without additional Sn, this indicates that the result of process (B) can be further optimized (see SI Figure S5 and discussion therein). However, processes (A) and (B) allow the direct comparison of a process with and without additional Sn. The result clearly shows the beneficial effect of a Sn source during the absorber formation.

We discuss the physicochemical reason in the following. It is known that annealing a $\text{Cu}_2\text{ZnSnS}_4$ film in vacuum to $500 \text{ }^\circ\text{C}$ or higher leads to decomposition. Weber et al. showed that CZTS decomposes into solid Cu_2S and ZnS .⁴ They imply that volatile SnS and S were lost from the sample. According to this reaction the loss of Sn proceeds via desorption of SnS(e). SnS and SnSe are materials with a significant vapor pressure above $400 \text{ }^\circ\text{C}$.^{12,13} The proposed decomposition reaction occurs in vacuum, and the volatile species condense on the cold walls, i.e. the process is far from equilibrium. However, if conditions are such that an equilibrium can be reached, the decomposition reaction stops as soon as the partial pressures of the volatile products reaches the saturation pressure p_V . The solid compound is then in a dynamic equilibrium with its vapor. Equation 1 illustrates the new proposed stoichiometric chemical equilibrium reaction, based on the decomposition reaction described by Weber,⁴ however, now indicating that, given high enough pressure of the gas products, the reaction will proceed toward CZTS(e) (illustrated by \rightleftharpoons).



From eq 1 we deduce that in experiment (A) the loss of SnS(e) is not compensated by any significant SnS(e) partial pressure which leads to a loss of Sn from the surface region (see Figure S1 in SI for surface morphologies of annealed films). Clearly, the electronic structure of a Sn-depleted surface is not favorable for the formation of the p/n junction, as indicated by the poor efficiency obtained by process (A). In experiment (B) the additional Sn is quickly transformed in the presence of S into SnS(g) which supplies the necessary p_V right from the beginning of the annealing process. As a result, the decomposition of the CZTS(e) is inhibited.

On the basis of eq 1 it could be assumed that an excess S(e) atmosphere would also stop the decomposition reaction. However, the necessary partial pressure of S(e) is very high, as can be inferred from the decomposition of $\text{SnS}_2 \rightarrow \text{SnS}(\text{s}) + 1/2 \text{S}_2(\text{g})$, which has a saturation partial pressure of S_2 of $\sim 10^{-1} \text{ mbar}$ at $550 \text{ }^\circ\text{C}$ compared to $\sim 10^{-3} \text{ mbar}$ in the case of $\text{SnS}(\text{s}) \rightarrow \text{SnS}(\text{g})$.¹³ Furthermore, the elemental S(e) in the annealing box will mostly form $\text{S}(\text{e})_8$ rings, which are not suitable to balance the pressure of reactive $\text{S}(\text{e})_2$. Therefore, the only way to reach equilibrium is to supply SnS(e) or reactive $\text{S}(\text{e})_2$ in order to quickly reach p_V , which will prevent the decomposition reaction shown in eq 1.

From the presented solar cell results we conclude that the control of Sn losses is a prerequisite to form decent solar cells. In this case it is accomplished by introducing elemental Sn in the presence of S(e) into the annealing volume. They form a partial pressure of volatile SnS(e) and prevent the decomposition. The equilibrium in eq 1 is then shifted toward the reactant side, i.e. toward CZTS(e). The control of this equilibrium is the key to high-quality CZTS(e) films.

To investigate the equilibrium we have performed a series of annealing experiments, starting from a stack of only Cu and Zn which has been electrodeposited onto Mo-coated glass. The thicknesses of the Cu and Zn layers are chosen so that they are suitable to form CZTS.

The three annealing experiments described in the following are made in series from a single sample. A first annealing denoted as (I) is performed in a sulfur atmosphere at a temperature of $560 \text{ }^\circ\text{C}$ for 120 min to form $\text{Cu}_x\text{S} + \text{ZnS}$. Consequently, annealing (I) yields a sample equivalent to the right-hand side of eq 1 except for the absent gas-phase species, SnS and S_2 . The second heat treatment denoted as (II) is performed in a sulfur and SnS atmosphere at a temperature of $560 \text{ }^\circ\text{C}$ for 120 min to form CZTS and to drive the reaction to the left-hand side of eq 1. In this case the supply of SnS(g) is realized by introducing SnS₂ powder into the box. The solid SnS₂ is known to quickly decompose into $\text{SnS}(\text{g}) + 1/2 \text{S}_2(\text{g})$.¹³ In the third experiment (labeled (III)) the $\text{Cu}_2\text{ZnSnS}_4$ thin film is annealed in vacuum at a temperature of $560 \text{ }^\circ\text{C}$ for 6 h. According to eq 1 the thin film should decompose into Cu_xS and ZnS. The samples have been investigated by grazing incidence X-ray diffraction (XRD) and energy and wavelength dispersive X-ray mappings (EDX/WDX). Figure 2a,b depicts the XRD analysis of different heating steps, while EDX mapping results are shown in Figure 2c–h. In the first annealing (I) reflections originating from ZnS and Cu_9S_5 , i.e. a Cu-poor Cu_2S , are identified. Moreover, the Mo substrate (denoted by *) and a small contribution of MoS_2 (labeled by #) are found. WDX analysis yields a Cu/Zn composition of 1.6. EDX mapping of the surface shown in Figure 2c enables us to analyze the lateral distribution of the Cu_xS and ZnS grains. The X-rays originating from Cu are color-coded in red, whereas those from Zn are colored in green. No intermixing of the Cu and Zn signal occurs since only red and green are visible after addition of the two EDX images. This is confirmed in Figure 2d where an EDX linescan is shown. It is clearly visible that the Cu and Zn signals are anticorrelated which means that Cu_9S_5 and ZnS do not intermix. In the XRD analysis of annealing (II), where SnS was present during the heat treatment, no indication of a Cu_xS is visible anymore as shown in Figure 2a. Moreover additional reflections corroborate that CZTS has been formed (see $2\theta = 29.7^\circ, 37^\circ, 38^\circ, 45^\circ$). Since the main reflexes of ZnS and CZTS are very close (see $2\theta = 28.5^\circ$ and 47.3°), we cannot exclude remaining ZnS that has not been transformed into CZTS. However, the small shift toward lower angles shown in Figure 2b confirms that the majority of the ZnS has been consumed. This is also apparent in Figure 2e and f where the EDX signals of Cu, Zn, Sn show a strong correlation in complete contrast to Figure 2c where Cu and Zn showed a strong anticorrelation. Even more interesting is that the resulting WDX elemental ratios, $\text{Cu}/(\text{Zn} + \text{Sn}) = 0.78$ and $\text{Zn}/\text{Sn} = 0.97$, are very close to the optimum values for high-performance solar cell absorbers. This shows that the incorporation of Sn via SnS does not proceed in a random way but is self limiting. As long as enough Cu_xS and ZnS is present, SnS and S from the gas phase are incorporated in the film to form

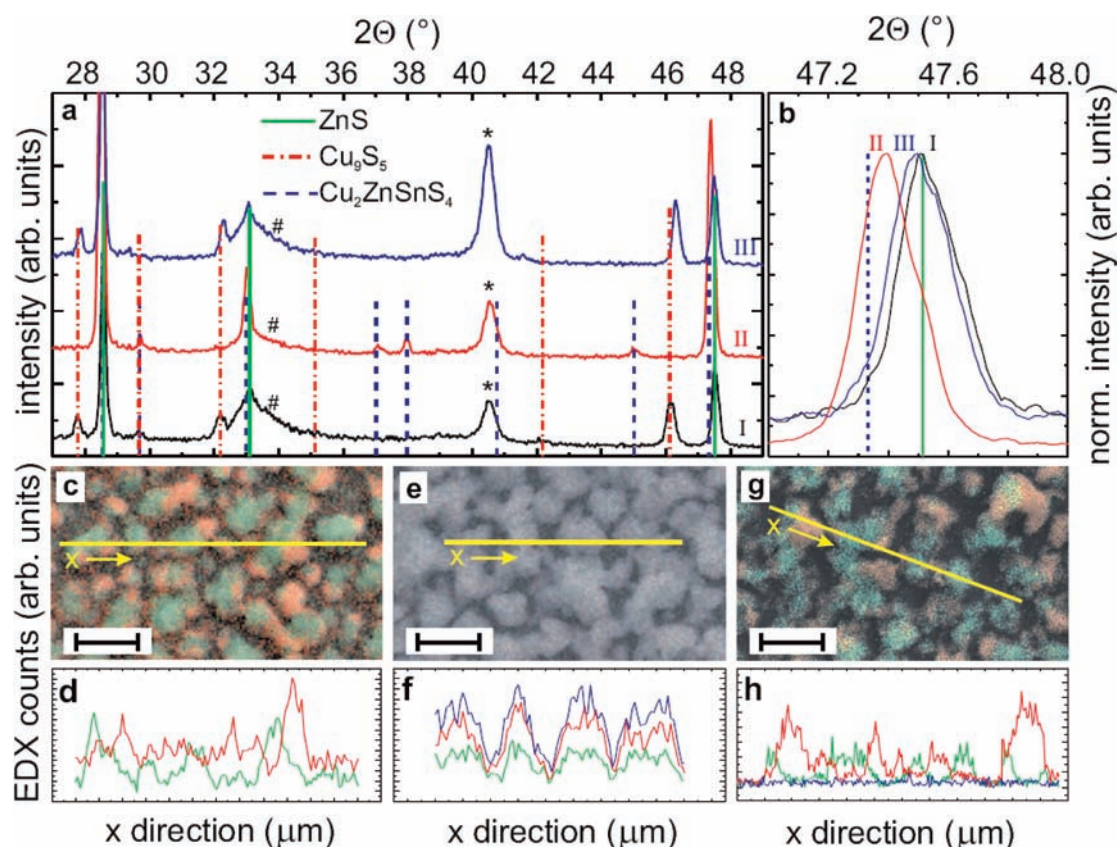


Figure 2. (a) Grazing incidence X-ray diffraction pattern of three different annealing experiments which elucidate the equilibrium proposed in eq 1. Scan (I): after annealing of a Cu/Zn stack in sulfur. Scan (II): after annealing of a mixed Cu_9S_5 and ZnS film in sulfur and $\text{SnS}(\text{g})$. Scan (III): after annealing CZTS in vacuum. Identified phases: --- (green) S, - - - (red) Cu_9S_5 , - - - (blue) $\text{Cu}_2\text{ZnSnS}_4$, (*) Mo substrate, (#) MoS_2 (JCPDS pattern indicated in SI). (b) Enlarged view of $47.2\text{--}48^\circ$ to demonstrate clear differentiation of CZTS and ZnS. (c, e, g) EDX topview mappings: red \equiv Cu, green \equiv Zn, blue \equiv Sn; details, see text. (c) Corresponds to process (I), (e) corresponds to process (II), (g) corresponds to process (III). (d) Linescan indicated in c, (f) linescan indicated in e, (h) linescan, indicated in g. The bars in SEM images equal $3\ \mu\text{m}$.

CZTS. This model experiment shows that eq 1 can be used to form CZTS by controlling the partial pressures of the volatile species. In the presented case the presence of a Sn source drives the reaction toward the CZTS side. Of course the situation can be reversed by taking the finished CZTS absorber and repeating the annealing process for a third time without additional S or SnS_2 in the box. The heating (III) has been performed under vacuum to reduce the S and SnS partial pressures to a minimum. After 6 h of heating the CZTS has been transformed back into Cu_9S_5 and ZnS as shown by the XRD analysis (Figure 2a). A Sn concentration of only 0.2 at % is identified by WDX analysis, and the mapping depicted in Figure 2g,h shows again anticorrelated Cu and Zn signals.

On the basis of the equilibrium in eq 1 we predict that, to avoid Sn loss and achieve high-quality absorbers and surfaces, (i) excess $\text{SnS}(\text{e})$ has to be present during the final heat treatment of any precursor annealing process of kesterite absorbers, (ii) a coevaporation process requires high partial pressure of $\sim 10^{-3}$ mbar of $\text{SnS}(\text{e})$, (iii) reactive $\text{S}(\text{e})_2$ species from a cracker source will not provide a high enough partial pressure to avoid Sn loss. These predictions are in part confirmed by those processes that have achieved reasonably efficient kesterite solar cells so far; a very fast coevaporation process⁸ or a very short annealing process^{1,7} minimize the time available for the decomposition reaction and thus reduce Sn loss. Annealing in H_2S ⁹ can provide a sufficiently high partial pressure of S radicals via the decomposition of H_2S driving reaction 1 toward CZTS.

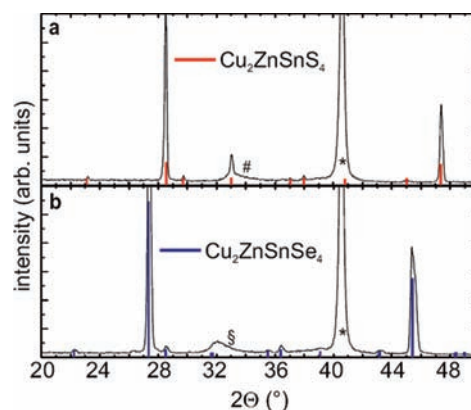


Figure 3. X-ray diffraction patterns of CZTS (a) and CZTSe (b). (a) Cu/Zn stack annealed with S and SnS_2 pellets. Most peaks can be identified with the $\text{Cu}_2\text{ZnSnS}_4$ kesterite phase (--- [red]). Moreover Mo (denoted as *) and a small contribution of MoS_2 (denoted as #) is identified. (b) Cu/Zn stack annealed with Se and SnSe_2 pellets. Reflections can be assigned to CZTSe (--- [blue]), Mo and MoSe_2 (denoted as S). EDX/WDX data and SEM images can be found in SI Table 2 and Figure S4.

A further prediction is that the self-regulating nature of the Sn incorporation can be used to drastically simplify the preparation process. Figure 3 shows the result of a process where a Cu/Zn

stack is annealed directly in (a) S and SnS₂ and in (b) Se and SnSe₂. The XRD analysis corroborates in both cases that the quaternary semiconductor has been formed. All reflections can be identified with CZT(S,Se) except Mo and MoS(e)₂ which originate from the substrate. EDX results (see Supporting Information Table 3) show again that the incorporation proceeds in a self-limiting way. No secondary phase can be detected by XRD. The small difference in the lattice constant of the CZTSe compared to the literature values is due to a small amount of S which was still present in the annealing furnace and was consequently incorporated into the film.

In conclusion we showed that understanding the growth reaction for the formation of CZTS(e) is the key to dramatically improve the solar cell efficiency. The Sn losses have to be controlled in order to form a high-quality semiconductor surface. Incorporating excess Sn + S(e) to the annealing environment improves the solar cell efficiency significantly and reproducibly. Moreover, the presented findings offer a unique possibility to produce CZT(S,Se) thin film absorbers on the basis of a very simple precursor, namely a Cu/Zn stack and one annealing step. The final composition of the CZTS can be governed simply by controlling the Cu/Zn ratio in the precursor since Sn and S are included in a self-controlled way. The described equilibrium reaction shown in eq 1 is valid for CZTS, CZTSe, and mixed CZTS(e) thin films, and the four-dimensional parameter space spanned by four elements can be reduced to two dimensions.

■ ASSOCIATED CONTENT

S **Supporting Information.** Detailed description of experimental methods, SEM micrographs of films annealed under different conditions, quantum efficiency spectrum and solar cell parameters, compositional details, comparison with previous solar cell results. This material is available free of charge via the Internet at <http://pubs.acs.org>.

■ AUTHOR INFORMATION

Corresponding Author
dominik.berg@uni.lu

■ ACKNOWLEDGMENT

We acknowledge the use of the SEM and XRD apparatus through the CRP Gabriel Lippmann (Luxembourg), the Helmholtz Zentrum Berlin for finishing the solar cell devices, Yasuhiro Aida for CdS deposition, and Guillaume Zoppi for the supply of Mo-coated glass substrates. Funding through TDK Corporation in the framework of the TDK Europe Professorship and FNR Luxembourg via the research projects C08/MS/20 (KITS) and ATTRACT/07/06 (PECOS) is acknowledged.

■ REFERENCES

- (1) Todorov, T.; Reuter, K. B.; Mitzi, D. B. *Adv. Mater.* **2010**, *22*, E156.
- (2) Friedlmeier, T. M.; Wieser, N.; Walter, T.; Dittrich, H.; Schock, H. W. 14th European Photovoltaic Solar Energy Conference, Barcelona, 1997, *Proceedings of the 14th European Photovoltaic Solar Energy Conference*; Stephens and Assoc.: Barcelona, 1997; p 1242.
- (3) Ahn, S.; Jung, S.; Gwak, J.; Cho, A.; Shin, K.; Yoon, K.; Park, D.; Cheong, H.; Yun, J. H. *Appl. Phys. Lett.* **2010**, *97*, 021905.
- (4) Weber, A.; Mainz, R.; Schock, H. W. *J. Appl. Phys.* **2010**, *107*, 013516.

- (5) Redinger, A.; Siebentritt, S. *Appl. Phys. Lett.* **2010**, *97*, 092111.
- (6) Lewis, N. S. *Science* **2007**, *315*, 798.
- (7) Wang, K.; Gunawan, O.; Todorov, T.; Shin, B.; Chey, S. J.; Bojarczuk, N. A.; Mitzi, D.; Guha, S. *Appl. Phys. Lett.* **2010**, *97*, 143508.
- (8) Schubert, B. A.; Marsen, B.; Cinque, S.; Unold, T.; Klenk, R.; Schorr, S.; Schock, H. W. *Prog. Photovoltaics: Res. Appl.* **2011**, *19*, 93.
- (9) Katagiri, H.; Jimbo, K.; Yamada, S.; Kamimura, T.; Shwe Maw, W.; Fukano, T.; Ito, T.; Motohiro, T. *Appl. Phys. Express* **2008**, *1*, 041201.
- (10) Probst, V.; Palm, J.; Visbeck, S.; Niesen, T.; Tolle, R.; Lerchenberger, A.; Wendl, M.; Vogt, H.; Calwer, H.; Stetter, W.; Karg, F. *Sol. Energy Mater. Sol. Cells* **2006**, *90*, 3115.
- (11) Patent filed at the Luxembourg Patent Office, LU 91754, on 18 November 2010.
- (12) Zocchi, F.; Piacente, V. *J. Mater. Sci. Lett.* **1995**, *14*, 235.
- (13) Piacente, V.; Foglia, S.; Scardala, P. *J. Alloys Compd.* **1991**, *177*, 17.